MIE 610: Nonlinear Dynamics Final Project

Jason Pettinato

12/05/2024

Abstract

This paper will look at and implement the dynamical system presented in a research article by Panagitotis Alevras, Stephanos Theodossiades, and Homer Rahnejat called 'On the dynamics of a nonlinear energy harvester with multiple resonant zones'. This work models the motion of a magnet suspended between two stationary magnets which create motion using magnetic flux induced by rotation of a motor. The original work uses harmonic balancing and numerical analysis to understand the dynamics of a nonlinear vibration energy harvester subjected to constant rotation. This work will investigate the chaotic behaviors, bifurcations, and any other nonlinear phenomena that the system exhibits, and compare the findings to what was discussed in the original work. Secondarily, the Sprott system J was investigated for chaotic behavior.

1 Introduction

Harvesting energy from motion is a difficult challenge that has a wide range of applications in energy and transportation. Scientists are still studying how energy can be efficiently be extracted from systems by taking advantage of resonant zones. This paper will investigate the nonlinear dynamics of a oscillatory energy harvester presented by Alevras and others [1].

This system is a simple oscillator developed to understand how kinetic energy of a magnet can be efficently extracted using principles of magnetic-induced voltage differences. The authors use an existing simplification developed in [3] to represent the stationary magnet's force on the levitating magnet using a 3rd order polynomial. This simplification enables nonlinear dynamic analysis of the system, including frequency methods which are out-of-scope for this project.

The primary goal of this work is to model this system based on the information provided in [1], and investigate how changing experimental parameters will lead to bifurcations and chaotic behavior. Furthermore, analytical solutions of the system are investigated while omitting functions of time in the equation of motion.
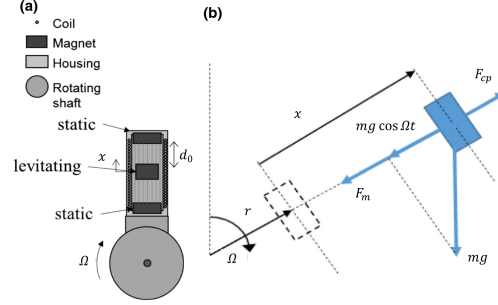
Figure 1: System model (a) and free body diagram (b) for the energy harvester [1]

2 Equations

The equation of motion for the system was derived using a 3rd order polynomial approximation of the magnetic forces acting on the system [3] $F_m(x) = kx + k_3 x$. A secondary force from the magnet rotation was also included as $F_{cp} = m\Omega(r + x)$, where r is the distance from the rotating magnet to the suspended mass.

Using some assumptions about system behavior, such as the presence of gravity and non viscous damping, the authors obtain a second-order ODE which fully describes the motion of the mass suspended by the magnetic field.

$$m\ddot{x} + c_m\dot{x} + kx + k_3x^3 = m\Omega^2(r + x) - mg\cos(\Omega t) \tag{1}$$

After normalizing with $\omega_n^2 = k/m, \beta = k_3/m, c_m/m = 2\zeta\omega_n$

$$\ddot{x} + 2\zeta\omega_n\dot{x} + (\omega_n^2 - \Omega^2)x + \beta x^3 = \Omega^2 r - g\cos(\Omega t) \tag{2}$$

A term $\dot{x}\frac{c_{el}}{m}$ is added to represent the force generated by the current flowing through the coil e.g. Faraday's law. This results in the final equation of motion:

$$\ddot{x} + \dot{x}\left(2\zeta\omega_n + \frac{c_{el}}{m}\right) + (\omega_n^2 - \Omega^2)x + \beta x^3 = \Omega^2 r - g\cos(\Omega t) \tag{3}$$

The system is decoupled into two first-order ODEs for analysis using $\dot{x} = y$

$$= \begin{cases} \dot{x} = y \\ \dot{y} = -y\left(2\zeta\omega_n - \frac{c_{el}}{m}\right) - (\omega_n^2 - \Omega^2)x - \beta x^3 + \Omega^2 r - g\cos(\Omega t) \end{cases} \tag{4}$$

If desired, the static equilibrium of the system can be studied by ignoring the terms which are functions of time, giving:

$$= \begin{cases} \dot{x} = y \\ \dot{y} = -y\left(2\zeta\omega_n - \frac{c_{el}}{m}\right) - (\omega_n^2 - \Omega^2)x - \beta x^3 + \Omega^2 r \end{cases} \tag{5}$$

The definitions and values are:

Parameter	Value	Units	Description
Ω	10	rad/s	Rotational speed (parameter)
r	0	m	Eccentric radius (parameter)
ω_n	89	rad/s	Natural resonant frequency
g	9.81	m/s^2	Gravitational acceleration
ζ	0.03	$-$	Damping ratio
c_{el}	0.0456	Ns/m	Electrical damping coefficient
m	0.02	kg	Mass
k_3	7×10^5	N/m^3	Nonlinear stiffness coefficient
β	$\frac{k_3}{m} = 3.5 \times 10^7$	s^{-2}	Nonlinear stiffness term
x	$-$	m	Displacement of the mass
y	$-$	m/s	Velocity of the mass (substituted as $\dot{x}$)

Finally, it is important to discuss what parameters will be investigated - and what that will physically mean. The most obvious terms to very are Ω, r, as these could very easily changed when conducting experiments. Something potentially more interesting is

3 Results

3.1 Fixed Points

Across all experiments, $0 \leq r \leq 0.006$. Values of Ω are not provided, but the values are constant and are assumed to be in the range of $[0, 500]\frac{rad}{s}$. In order to avoid frequency response analysis, which was done in the paper, the forcing term $gcos(\Omega t)$ is omitted. For the given system parameters, there are no positive fixed points. The system must satisfy $\dot{y}, \dot{x} = 0$, and this results in a cubic system with no positive solutions for the chosen parameters. More information in the discussion.

3.2 Bifurcation Points

Because our system, equation (5), is a cubic - we are interested in seeing when the system undergoes a transition from imaginary to real roots. Since bifurcations occur at fixed points, we set $y = 0$.

$$\dot{y} = -(\omega_n^2 - \Omega^2)x - \beta x^3 + \Omega^2 r = 0$$

For a cubic system, the transition from real to imaginary solutions is dependent on the discriminant, Δ, which takes the form $b^2c^2 - 4ac^3 - 4b^3d - 27a^2d^2 + 18abdc$. Note, however, that this cubic is depressed because $b = 0$. The discriminant is $-4ac^3 - 27a^2d^2$ which gives:

$$\Delta = -4(\beta)(\omega_n^2 - \Omega^2)^3 + 27(\beta^2)(\Omega^2 r)$$

3

When $\Delta = 0$, there is bifurcation. Expanding this equation gives:

$$\Delta = -4\omega_n^6 + 12\omega_n^4\Omega^2 - 12\omega_n^2\Omega^4 + 4\Omega^6 + 27\beta\Omega^2 r = 0$$

Since this is a 6th order polynomial in both Ω, there is no analytical solution for when these parameters will make the system bifurcate. However, it is still possible to use numerical methods to solve for this. The results of these numerical methods can be found below.
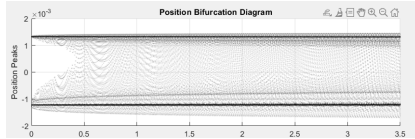
3.3 Bifurcation Diagram

In the experiment, the researchers varied the frequency of oscillation Ω, and the radius r across different trials. Furthermore, β is also chosen as a parameter of interest because it can be changed by changing the mass of the oscillator. It would also be feasible to control the natural frequency of the system, ω_n, so this parameter was varied as well. Initially, the radius r was investigated for bifurcation behavior, but nothing of interest was found. In all, the following parameters are varied for bifurcations: Ω, ω_n, β

The system was modeled in Matlab and solved using ODE15 since the system is relativey stiff. The transients of the system quickly died out after 3 seconds, so the simulation data shown is for $t = (3, 10)s$. The number of points per simulation was varied between $n = (1000, 25000)$ depending on the range of the bifurcation parameter, and empirical analysis of plot behavior.

The findpeaks function in Matlab was used to find when $\dot{x}, \dot{y} = 0$, indicating bifurcation. There is quite a lot of noise in the plots, and some sinusoids pass through the primary roots of 2 which appears to be something like a pitchfork bifurcation.

It is possible that the faint lines appearing in many of these plots are hints of instability. A more thorough investigation into unstable fixed points may be necessitated for more conclusive results.

Finally, it is important to note that in the reference paper, there is significant effort put into frequency response analysis. The apparent noise in these figures may disappear when proper frequency analysis is done, giving much cleaner plots as seen in the original paper.
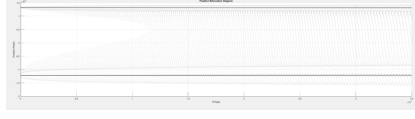

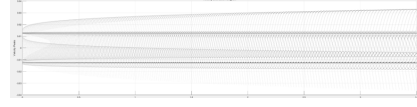(a) Position diagram under forced conditions.
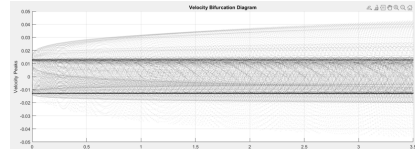
(b) Velocity diagram under forced conditions.

Figure 2: Bifurcation diagrams for $\beta \in [0, 3.5 \cdot 10^5]$ under forced conditions.

(a) Position diagram under non-forced conditions.

(b) Velocity diagram under non-forced conditions.

Figure 3: Bifurcation diagrams for $\beta \in [0, 3.5 \cdot 10^5]$ under non-forced conditions.

4 Discussion

4.1 Fixed Points: Analytical Solution

The fixed points of the system are for all $y = 0$, and the values of x that give a fixed point x^* are given by the solutions to the cubic equation. To solve the cubic equation, let us write out the expression we want to find the roots of:

$$\dot{y} = -(\omega_n^2 - \Omega^2)x - \beta x^3 + \Omega^2 r = 0$$

Since there is no x^2 term, the system can easily be decomposed into a depressed cubic which takes the form $x^3 + px + q = 0$:

$$x^3 + \frac{\omega_n^2 - \Omega^2}{\beta}x + \frac{\Omega^2 r}{\beta} = 0$$

Next, write $A = \frac{\omega_n^2 - \Omega^2}{\beta}, B = \frac{\Omega^2 r}{\beta}$. For a cubic system, we look at the discriminant D to determine the number of roots.

$$D = \left(\frac{B}{2}\right)^2 + \left(\frac{A}{3}\right)^3$$

For $D < 0$, there three non equal real roots. $D = 0$ has all real roots, with at least two being equal. $D > 0$ has one real root and two complex roots.

For the first case, look at $D > 0$:

$$S = \sqrt{D} \quad u = \left(-\frac{B}{2} + S\right)^{1/3} \quad v = \left(-\frac{B}{2} - S\right)^{1/3}$$

The real root is then $x = u + v$

For the second case, look at $D = 0$.

$$u = \left(-\frac{B}{2}\right)^{1/3}, x_1 = 2u_1, x_2 = -u$$

For the third case: $D < 0$

$\theta = arccos\left(-\frac{B}{2} / \sqrt{-\left(\frac{A}{3}\right)^3}\right)$ The roots for this are given by

$$x_k = 2\sqrt{-\frac{A}{3}} \cos\left(\frac{\theta - 2\pi k}{3}\right), k = 0, 1, 2$$

All terms present β, r, Ω are parameters that can be varied in the experimental setup. However, β is a function of mass, and so is ω_n, and potentially other terms. Because it was not stated how ω_n was found, varying the bifurcation parameter β requires that the nonlinear stiffness coefficient k_3 is changed instead. This is feasible by changing the strength of the magnets.

In order to get some value for x^*, the numbers in Table 1 are used to solve for A and B:

$$A = \frac{89^2 - 10^2}{3.5 \cdot 10^7} = 2.23 \times 10^{-4},$$
$$B = \frac{10^2 \cdot 0.006}{3.5 \cdot 10^7} = 1.71 \times 10^{-8}.$$

$$D = 4.13 \times 10^{-13}$$

So, $D > 0$ and there is one real root. We can solve for u, v to get x. After solving, $x = -7.67 \times 10^{-5}$. There is no physically meaningful fixed point for the system parameters used in the experiment.

4.2   Bifurcations

Looking at bifurcations, we are primarily interested in the roots of the discriminant equation when inspecting different bifurcation parameters. As shown in section 3, the discriminant has the expanded form

$$\Delta = -4\omega_n^6 + 12\omega_n^4\Omega^2 - 12\omega_n^2\Omega^4 + 4\Omega^6 + 27\beta\Omega^2 r = 0$$

As previously stated, the system is quartic with respect to ω_n, Ω. However, β, r can be solved for very simply. It is *very* unlikely that r will bifurcate within the range of experimental values $r \in [0, 0.006]$, thus β will only be considered.

$$\beta = \frac{4\omega_n^6 - 12\omega_n^4\Omega^2 + 12\omega_n^2\Omega^4 - 4\Omega^6}{27\Omega^2 r}$$

Beta leads to bifurcation when $\Omega < \omega_n$. This was done by varying values. r never leads β to bifurcation. This result is quite clear when looking at the discriminant equation before is was expanded.

4.3   Classifying Fixed Points

The classification of fixed points is performed by linearization at the location of the fixed point using the Jacobian matrix $\mathbf{A}$. The formula for the Jacobian is given as:

$$\mathbf{A} = \begin{bmatrix} \frac{\partial f}{\partial x} & \frac{\partial f}{\partial y} \\ \frac{\partial g}{\partial x} & \frac{\partial g}{\partial y} \end{bmatrix}$$

Using the system defined in (5) we get:

$$\mathbf{A} = \begin{bmatrix} 0 & 1 \\ -\omega_n^2 + \Omega^2 - 3\beta x^2 & -2\zeta\omega_n + \frac{c_{el}}{m} \end{bmatrix} \tag{6}$$

Using the fact that the trace and discriminant describe fixed point behavior, we find them as:

$$tr(A) = -2\zeta\omega_n + \frac{c_{el}}{m}$$

$$\Delta(A) = -(-\omega_n^2 + \Omega^2 - 3\beta x^2)$$

The fixed point behavior is described by

$$\tau - 4\Delta = \frac{c_{el}}{m} - 2\zeta\omega_n - 4 \cdot (\omega_n^2 - \Omega^2 + 3\beta x^2) \tag{7}$$

The type of fixed point (saddle, star, center) is not determined by r, but is instead only controlled by Ω, β. It is algebraically cumbersome to express x using the solution of the cubic equation in (7), and it is not practically useful.

However, we can observe the general behavior of the system based on this equation. When $\Delta < 0$, there is a saddle node. Using (15), this means

$$\omega_n^2 - \Omega^2 + 3\beta x^2 < 0 \tag{8}$$

For other cases, such as centers, spirals, or repelling/attracting nodes (16) is greater than 0. In this case, the value of τ will determine the types of fixed points.

To determine fixed point stability, the eigenvalues of the Jacobian must be determined. To find these, the solution of the expression $A - \lambda I = 0$ is solved.

Using

$$\mathbf{A} = \begin{bmatrix} 0 & 1 \\ -\omega_n^2 + \Omega^2 - 3\beta x^2 & -2\zeta\omega_n + \frac{c_{el}}{m} \end{bmatrix} \tag{9}$$

We can find that

$$\lambda = \frac{\frac{c_{el}}{m} - 2\zeta\omega_n \pm \sqrt{4\zeta^2\omega_n^2 \frac{c_{el}}{m} + \frac{c_{el}^2}{m^2} - 4(\omega_n^2 - \Omega^2 + 3\beta x^2)}}{2} \tag{10}$$

$$\lambda = -1.53 \pm \sqrt{70.1 - 4(7,921 - \Omega^2 + 105 \times 10^6 x^2)} \tag{11}$$

When both eigenvalues for some fixed point x^* are negative, then the system has reached equilibrium. In other words,

$$0 < \sqrt{70.1 - 4(7,921 - \Omega^2 + 105 \times 10^6 x^2)} < 1.53$$

There is no solution for this. This makes sense, as the system should never stop oscillating because of the continuous nature of this energy harvesting system.
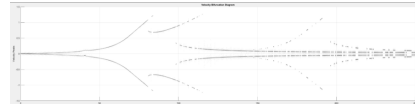
4.4 Chaotic Behavior

As a reminder, the system's equation of motion is given by:

$$\ddot{x} + \dot{x}\left(2\zeta\omega_n + \frac{c_{el}}{m}\right) + (\omega_n^2 - \Omega^2)x + \beta x^3 = \Omega^2 r - g\cos(\Omega t) \qquad (12)$$

The term that was previously omitted for simplicity, $g\cos(\Omega t)$, may cause chaotic behavior or attractors. The following figures are orbit diagrams for the case of a forced output, while varying either $\beta, \Omega, r, \omega_n$.
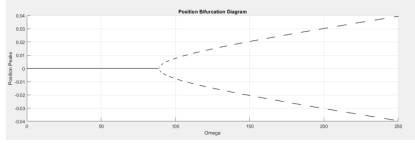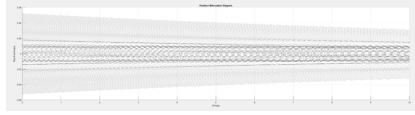

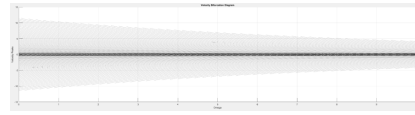(a) Position diagram under forced conditions.

(b) Velocity diagram under forced conditions.

Figure 4: Bifurcation diagrams for $\Omega \in [0, 250]$ under forced conditions.

(a) Position diagram for ω_n.

(b) Velocity diagram for ω_n.

Figure 5: Bifurcation diagrams for $\omega_n \in [0, 10]$ under forced conditions.

Generally, the system responses were quite stable, except for the results of the ω_n bifurcations in 5a. In these plots, the values of x that gave stability were apparently random (when x was in the range $[-0.02, 0.02]$)

Unsurprisingly, this response was during the forced oscillation conditions (when $g\cos(\Omega t)$ was present).

There was also strange 'bifurcation' behavior when Ω was subjected to forced conditions. These were not true bifurcations, because there was never a change in number of roots. Instead, the roots oscillated between negative and positive values while following a sadle node trajectory. The plots were constructed for n=30 initial conditions

The strange bifurcation occurred in 4b, where there are fragments in the continuity of the bifurcation after $\Omega = 100$. The reason for this is unclear, except that the increased energy may break down the model's accuracy, or this is simply when chaos begins. The trends of the curves in this plot are predictable, but the location that they exist does not seem to have any pattern.

5   Physics

As briefly described in the introduction, this system harvests the torsional vibrations of a magnet suspended between two stationary magnets. The rotation of a shaft at speed Ω introduces an oscillatory forcing function which makes the levitating magnet move between the stationary magnets. A coil is wrapped around the housing of the magnets, and the oscillation of the magnet is used to harvest its energy using principles of magnetic flux. As long as there is energy supplied to the system from the motor (simulating some form of vibration), the system will not stop. There can not be any stable fixed points.

The investigation of the system equations showed that there is a change in real roots of the system (via the discriminant) for some β when $\Omega < \omega_n$. This makes some physical sense. When the magnet is oscillating at a speed below the natural frequency of the system, the magnetic force is out-of-phase with the oscillation of the levitating magnet. This lag may lead to periods where there is a loss of energy, depending on the magnetic field strength (since the nonlinear stiffness coefficent k_3 largely determines β). In this case, the energies of the system may subtract from each other, leading to two zones where the magnet will stop in its motion.

6   Sprott System

The sprott system given is system J. It does not show particularly interesting behavior in comparison to other sprott systems. The equation for the system is

$$= \begin{cases} \dot{x} = az \\ \dot{y} = -by + cz \\ \dot{z} = -xd - ye - y^2 f \end{cases} \tag{13}$$

After reviewing literature, it appears that the parameters which lead to interesting chaotic behavior are a, b when they are near the value 2.

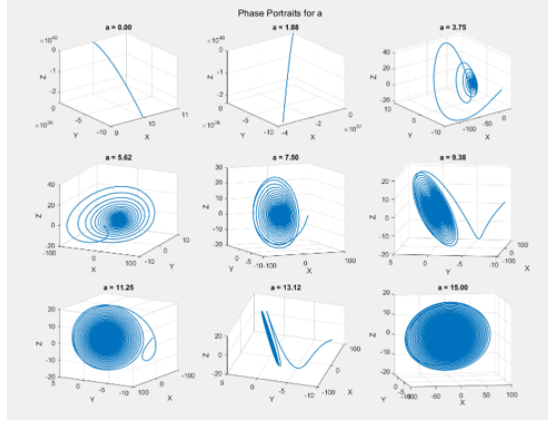Here are 3d phase portraits for the system when varying all parameters a, b, c, d, e, f:

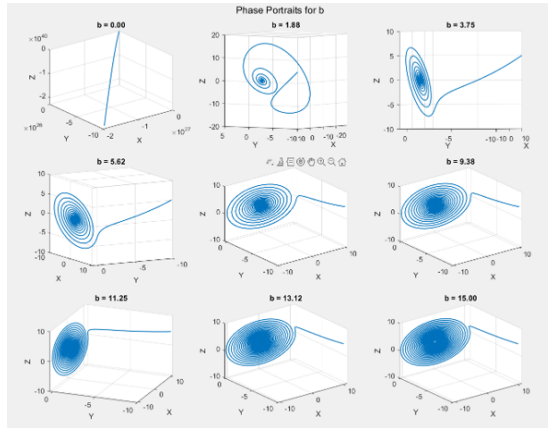Figure 6: Sprott system J for $a \in [0, 15]$

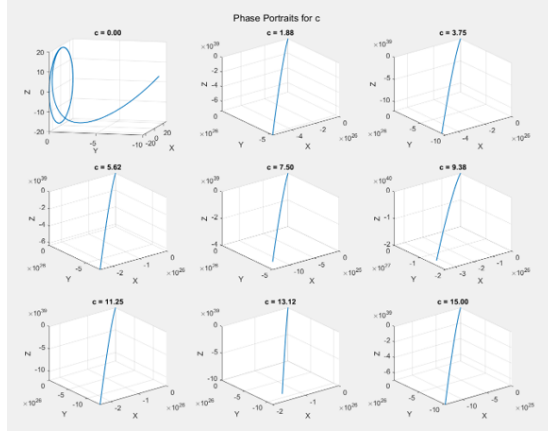Figure 7: Sprott system J for $b \in [0, 15]$

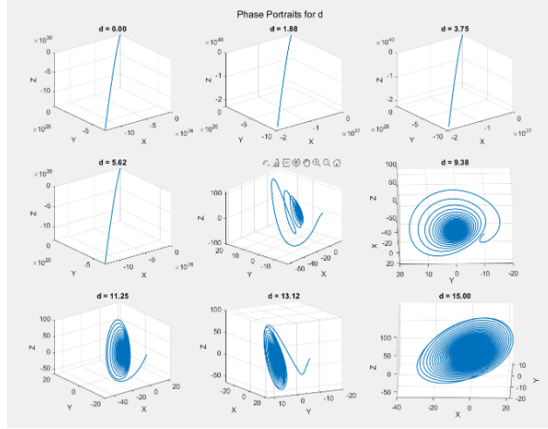Figure 8: Sprott system J for $c \in [0, 15]$
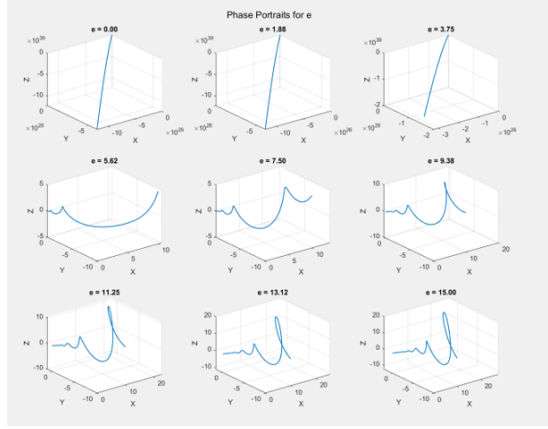

Figure 9: Sprott system J for $d \in [0, 15]$

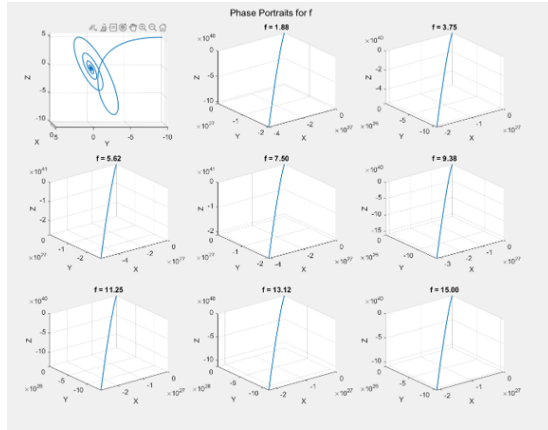Figure 10: Sprott system J for $e \in [0, 15]$

Figure 11: Sprott system J for $f \in [0, 15]$

As expected, the system does show some interesting behavior, and it occurs when the values a, b are varied. The system tends to be stable for large enough a, b. There is probably some relationship between all the parameters, and if the ratio of them to one another meets some condition, the attractor appears and the system cycles.

The system is generally not stable for the base initial conditions, which were set to be 0.5. There is unexpected behavior as e increases.

Below are the orbit diagrams for the system under varied initial conditions. Generally, the x axis shows the most interesting behavior, but there is apparent noise for the cases and the reason is not clear why. Simulation time was $t \in [0, 500]$, with only the last 10 percent of data being used in findpeaks. Perhaps the range of values in the sweep was too high for interesting behavior, or the

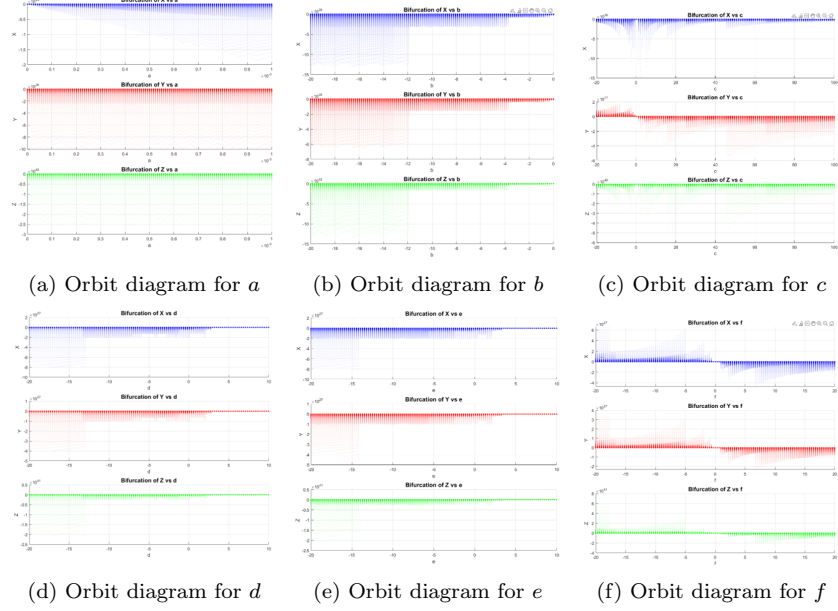base values for the other parameters not being varied are not good enough.

(a) Orbit diagram for a (b) Orbit diagram for b (c) Orbit diagram for c

(d) Orbit diagram for d (e) Orbit diagram for e (f) Orbit diagram for f

Figure 12: Sprott system J bifurcation diagrams for all parameters $a-f \in [0, 15]$

7   References

[1] Alevras, P., Theodossiades, S. Rahnejat, H. On the dynamics of a nonlinear energy harvester with multiple resonant zones. Nonlinear Dyn 92, 1271–1286 (2018). https://doi.org/10.1007/s11071-018-4124-2

[2] Sprott, J. C. "Some Simple Chaotic Flows". Physical Review E, vol 50, no. 2, 1994, pp. R647-R650. American Physical Society (APS), doi:10.1103/physreve.50.r647.

[3] Mann, B.P., Sims, N.D.: Energy harvesting from the nonlinear oscillations of magnetic levitation. J. Sound Vib. 329(9), 515–530 (2009). https://doi.org/10.1016/j.jsv.2008.06.011